DOI: 10.1002/ejic.200800214

Slow-Proton Dynamics within a Zirconium-Containing Sandwich-Like Complex Based on the Trivacant Anion α-$[SiW_9O_{34}]^{10-}$ – Synthesis, Structure and NMR Spectroscopy

Nathalie Leclerc-Laronze,[a] Jérôme Marrot,[a] Mohamed Haouas,[a] Francis Taulelle,[a] and Emmanuel Cadot*[a]

Keywords: Polyoxometalate / Zirconium / Tungsten / ^{183}W NMR spectroscopy

Reaction of $ZrOCl_2$ with the potassium tungstosilicate A-α-$[SiW_9O_{34}]^{10-}$ in water at pH = 4 leads to the formation of the sandwich-type complex $[Zr_3O(OH)_2(SiW_9O_{34})_2]^{12-}$ (**H_2-1**) which has been structurally characterised by single-crystal X-ray diffraction. It consists of a $[Zr_3O(OH)_2]$ triangular central cluster closely embedded between two A-α-$[SiW_9O_{34}]^{10-}$ subunits. Inspection of the geometric parameters within the $\{Zr_3O_3\}$ core unambiguously reveals the presence of two attached protons giving two hydroxo Zr–OH–Zr bridges and a single oxo Zr–O–Zr junction. The anions **H_x-1** with x = 3, 2 or 1 were obtained in solution at pH = 2, 4 and 7.5, respectively, and were subsequently characterised by ^{183}W and ^{29}Si NMR spectroscopy in aqueous solution. ^{183}W NMR spectra appear strongly dependent upon the protonation state of the trizirconium central core, $\{H_xZr_3O_3\}$. ^{183}W NMR spectroscopy of **H_2-1** gives a two-line spectrum, consistent only with the hopping of the two H^+ ions over the three bridging Zr–O–Zr oxygen atoms. Interestingly, the resonance attributed to the six tungsten atoms of the belt connected to the zirconium atoms through W–O–Zr junctions exhibits substantial line-broadening ($\Delta\nu_{1/2}$ = 21 Hz) interpreted as a slow dynamic process involving the H^+ ions. Such behaviour contrasts with the fast H^+ mobility generally observed in other POM systems and this will be discussed in relation to the peculiar environment of the $\{Zr_3O_3\}$ core which hinders structural relaxation consequent with the H^+ hopping. Both ^{183}W resonances of the **H_3-1** anion remain sharp as usual ($\Delta\nu_{1/2}$ = 1.6 Hz) consistent with the presence of the triprotonated species $[Zr_3(OH)_3(SiW_9O_{34})_2]^{11-}$ whereas for the monoprotanated anion (**H-1**), the resonance of the belt becomes broad enough to be indistinguishable. Infrared spectroscopy, elemental analysis, pH titration and polarographic measurements of **H_x-1** were also carried out.

Introduction

Polyoxometalates have attracted increasing attention with their interesting magnetic, (electro)catalytic properties and for applications in nanotechnology.[1] In such contexts, the use of vacant heteropolytungstate anions acting as multidentate rigid ligands has significantly enriched the possible combinations with metallic cations and permits the rational design of a myriad of compounds which are diverse in structure, composition and properties. They are often involved as soluble metal oxide supports for transition metal catalysts. Zirconium-based chemistry with polyoxometalates has been investigated for a long time since the first Zr-containing polyoxometalates (Zr–POM) were reported by Finke et al. in 1989.[2] Mainly driven by their catalytic properties, Zr substituted polyoxoanion chemistry remains actively studied, especially because of recent developments in their application as molecular materials which can be used for studying the Bayer–Villiger process of H_2O_2-based selective oxidation catalysis.[3] Furthermore, zirconium-substituted polyoxometalates provide useful structural models for the understanding, at the molecular level, of the functioning of zirconia-supported tungsten catalysts (WZ catalysts).[4] Since the first Zr-containing polyoxotungstate, $[Si_2W_{18}Zr_3O_{71}H_3]^{11-}$, numerous POM–Zr combinations have been characterised exemplifying the structural diversity mentioned above. Monovacant anions such as Keggin or Dawson derivatives generally lead to 2:1 complexes with an eight-coordinate central Zr^{IV} atom.[5] Similar arrangements can even be attained with the monovacant phosphomolybdate anion.[6] The situation can be quite a bit more complicated when divacant or trivacant anions are used, since isomerisation or rearrangement processes occur to give multiunit anions containing central polynuclear Zr–O cores. In the presence of the divacant γ-$[SiW_{10}O_{36}]^{8-}$ anion, asymmetric zirconium-substituted silicotungstates such as $[Zr_6O_2(OH)_4(H_2O)_3(\beta\text{-}SiW_{10}O_{37})_3]^{14-}$ and $[Zr_4O_2(OH)_2$-

[a] Institut Lavoisier de Versailles, ILV, UMR CNRS 8180, Université de Versailles Saint-Quentin-en-Yvelines,
45 avenue des Etats-Unis, 78035 Versailles Cedex, France
Fax: +33-1-39254381
E-mail: cadot@chimie.uvsq.fr

$(H_2O)_4(\beta\text{-}SiW_{10}O_{37})_2]^{10-}$ are obtained.[7] They are built up through the association of disubtituted β-isomer Keggin-derived β-$[SiW_{10}Zr_2O_{40}]^{8-}$. Condensation of Zr^{4+} cations on the trivacant Wells–Dawson anion $[P_2W_{15}O_{56}]^{12-}$ gives similar results. Rearrangement of the lacunary precursor produces the dimodular species $[Zr_4(\mu_3\text{-}O)_2(\mu_2\text{-}OH)_2(H_2O)_4(P_2W_{16}O_{59})_2]^{14-}$.[8] Recently, Hill's group put forward the chemistry of the POM–Zr systems with recent reports demonstrating the ability of the Zr centre to coordinate carboxylate ions within the polyoxometalate.[9] As a fruitful development of such a system, the use of chiral inductors such as D- or L-tartaric acid directs the Zr–POM condensation process toward the formation of the pure enantiomers $\{[\alpha\text{-}P_2W_{15}O_{55}(H_2O)]Zr_3(\mu_3\text{-}O)(H_2O)(X\text{-}tartH)[\alpha\text{-}P_2W_{16}O_{59}]\}^{15-}$ with X = D or L.[10] Furthermore, the same group provided new insight into the dynamics of the reversible protonation on polyoxoanion surfaces in the complexes $[\{P_2W_{15}O_{54}(H_2O)_2\}_2Zr]^{12-}$ and $[\{P_2W_{15}O_{54}(H_2O)_2\}Zr\{P_2W_{17}O_{61}\}]^{14-}$.[11] The richness of the Zr–POM chemistry is probably due to the versatile coordination sphere, as exemplified by a diunit Linqvist-type complex reported by Villaneau et al. in which seven-coordinate Zr atoms were observed.[12] A similar arrangement was found by Kholdeeva et al. within a Keggin-type dimer.[13] The $[Zr_2(\mu\text{-}OH)(H_2O)_2(AsOH)_2(AsW_7O_{28})(AsW_{10}O_{36})]^{9-}$ anion contains a mixing of six- and seven-coordinate Zr centres.[14] It should also be mentioned that the chemistry of zirconium substituted polyoxometalates offers the possibility of developing nonaqueous syntheses of Lindqvist-type alkoxo complexes, thus opening an attractive route for the synthesis of POM-based hybrids.[15] The discovery of new arrangements based on Zr–POM system can be achieved by the use of new polyvacant precursors. Recently, we have shown that acidification in aqueous solution of the trivacant anion A-α-$[SiW_9O_{34}]^{10-}$, as its potassium salt, leads to the formation of the dimeric tungstosilicate α-$[Si_2W_{18}O_{66}]^{16-}$ which exhibits a Wells–Dawson open structure.[16] This arrangement delimits a large central cavity which encloses a nonexchangeable potassium cation. We demonstrated that the dimeric anion α-$[\{K(H_2O)_2\}Si_2W_{18}O_{66}]^{15-}$ acts as a lacunary species and can bind several transition-metal cations such as VO^{2+}, Fe^{3+} and Co^{2+}.[17,18] Herein, we report on the reactivity of aqueous Zr^{IV} in the presence of the dimeric α-$[\{K(H_2O)_2\}Si_2W_{18}O_{66}]^{15-}$ anion. However, this system leads to the classical sandwich-type complex $[Zr_3O(OH)_2(SiW_9O_{34})_2]^{12-}$ (noted **H_2-1**). Structural determination of **H_2-1** reveals a diunit assembly built up from two $[SiW_9O_{34}]^{10-}$ subunits that retain the α isomerism instead of the β isomerism, previously described by Finke et al.[2] However, examination of bond geometric parameters, supported by bond valence sum calculations and elemental analysis, shows the presence of two protonated Zr–O–Zr bridges among the three present in **H_2-1**. ^{183}W NMR spectroscopic investigation of the anion at different protonation states (noted **H_x-1**, with x = 1, 2 or 3) in aqueous solution was undertaken. The ^{183}W NMR spectra exhibit striking differences related to the "net" hopping of the attached protons over the three Zr–O–Zr bridges. The slowness of the dynamic process observed in aqueous media can be interpreted as a slow structural relaxation of the $\{Zr_3O_3\}$ fragment consequent with the protonation process.

Results and Discussion

Synthesis

Zirconyl chloride was treated with α-$[\{K(H_2O)_2\}Si_2W_{18}O_{66}]^{15-}$, first formed in situ through acidification of K_{10}A-α-$[SiW_9O_{34}]\cdot 13H_2O$ at pH = 6.[19] Whatever the Zr/POM ratio and pH, dimeric associations **H_x-1** (with x = 1, 2 or 3) were obtained. This result contrasts with those obtained under similar conditions with Co^{2+}, VO^{2+} or Fe^{3+} cations where the resultant mixed compounds were based on the open Wells-Dawson arrangement.[17,18] Hence, the zirconyl cation seems to impose the stereochemistry of the condensation process. The anion **H_2-1** was isolated at pH = 4 as the cesium salt and recrystallised from sodium chloride solution in a moderate yield (ca 20%). Analytical characterisation of the single crystals (elemental analysis, protometric titration and TGA analysis) supported by the structure determination suggest the formula $Na_6Cs_6[Zr_3O(OH)_2(SiW_9O_{34})_2]\cdot 31H_2O$.

Molecular Structure

The discrete structure of **H_2-1** is depicted in Figure 1 (a) and corresponding relevant crystal data are given in the experimental section. The molecular structure of **H_2-1** consists of the association of two A-α-$[SiW_9O_{34}]^{10-}$ anions with three zirconium ions included, leading to a "sandwich" type complex $[Zr_3O(OH)_2(SiW_9O_{34})_2]^{12-}$. The anion **$H_2$-1** has the C_{2v} idealised symmetry rendering both superimposed A-α-$[SiW_9O_{34}]$ subunits equivalent. The relative orientation of the two associated anions is the same as that found in the compound A-α-$\{[Co(H_2O)_2]_3(SiW_9O_{34})_2\}^{14-}$.[19] The bond lengths and angles within the $\{SiW_9O_{34}\}$ subunit fall in the usual range generally observed for such structures. The geometrical arrangement of the three Zr atoms resembles that observed in the β-$\{SiW_9O_{34}\}$-based dimer.[2] Each zirconium cation is sandwiched between two ditungstic groups through four W–O–Zr bridges giving Zr–O bond lengths in the 2.08(2)–2.17(2) Å range (average 2.12 Å) and almost similar Zr–O–W angles (average 129 ± 1°). Besides, the three Zr atoms are mutually linked in the equatorial plane through three Zr–O–Zr junctions (see Figure 2). Thus, the three Zr atoms are six-coordinate and exhibit coordination geometries close to trigonal prismatic. Inspection of the bond lengths and angles of the Zr–O–Zr junctions provides evidence for the presence of two protons (see Figure 2). Indeed, the two junctions Zr1–O70–Zr2 and Zr2–O71–Zr3 display closed angles of 149.0(7)° and 147.9(7)°, respectively, while the Zr–O bond lengths for these junctions fall in the 2.11(2)–2.18(2) Å range (average 2.14 Å). These geometric parameters are close to those observed in the triprotonated anions previously reported by

Finke[2] and are consistent with protonated Zr–O–Zr bridges. The remaining Zr1–O69–Zr3 bridge appears significantly open [162.4(8)°] with shorter associated Zr–O bond lengths [1.96(2) and 1.97(2) Å, respectively], consistent with an unprotonated O69 atom. Bond Valence Sum calculation (BVS) for O(69–70–71) support this view. BVS values of 1.12 and 1.18 were found for the protonated O(70–71) oxygen atoms and 1.85 for the unprotonated O69 oxygen. Our conclusion about the presence of two protons is fully consistent with synthetic and crystallisation procedures (pH ≈ 4) while the triprotonated Zr–POM anion reported by Finke was obtained from solutions with pH < 2. Such results are supported by the pH titration of **H_2-1** which clearly indicates the pH domains of the tri-, di- and monoprotonated species based on the $\{H_xZr_3O_3\}$ fragments with x = 3, 2 or 1, respectively (see below). As a consequence of the triangular $\{Zr_3O_3\}$ arrangement, the Zr atoms are pulled towards the centre of the cluster (about 2.30 Å from the centre of the cluster) and then deviate by about 1 Å from the plane defined by their four coordinated oxygen atoms. Subsequently, each Zr atom makes two long and weak additional contacts with two oxygen atoms belonging to both SiO_4 tetrahedrons [2.81(2)–2.85(2) Å; average 2.82 ± 0.02 Å]. Furthermore, there are structural analogies between the anion **H_2-1** and the previously reported $K_9NH_4H_2[(A\text{-}\alpha\text{-}PW_9O_{34})_2(OCe)_3(OH_2)_2]\cdot 20H_2O$ compound.[20] Although the former has been isolated as single-crystals from a solution at pH = 2.6, the status of the distribution of its protons appears unclear and has not really been discussed. Our own analysis based upon the bond lengths and angles agrees with the presence of two protons attached to the $\{Ce_3O_3\}$ central core, one proton being unambiguously located at a bridging hydroxo group and the other equally distributed over the two remaining Ce–O–Ce bridges. Seemingly, in such a structure, the presence of two protons has a slight influence upon the coordination sphere of both involved Ce^{IV} atoms, each being coordinated to an additional terminal aqua ligand (seven-coordinated).

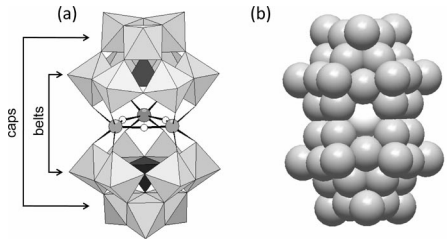

Figure 1. Structural description of **H_2-1** anion. a) Mixed polyhedral/ball-and-stick representation highlighting the $\{Zr_3O_3\}$ central cluster (ball-and-stick) sandwiched between both $\{SiW_9O_{34}\}$ subunits (polyhedra). b) Space-filling model showing the $\{Zr_3O_3\}$ core, closely embedded between both $\{SiW_9O_{34}\}$ moieties (grey spheres: oxygen atoms of the $\{SiW_9O_{34}\}$ subunits; white sphere: internal bridging oxygen atom of the $\{Zr_3O_3\}$ fragment).

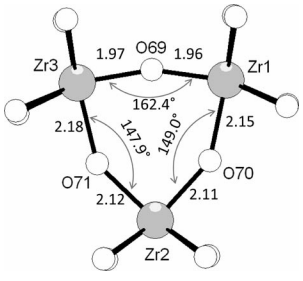

Figure 2. Isolated structural representation of the $\{Zr_3O_3\}$ cluster. The location of two protons on O70 and O71 is evidenced by the long Z–O bond lengths and the closed Zr–O–Zr angles.

Studies in Solution

Electrochemistry and Potentiometric Titration. The anion **H_2-1** was characterised in solution by its polarogram obtained in a 1 mol L^{-1} acetate buffer (pH = 4.8). The polarogram shows one wave at –0.92 V relative to the saturated AgCl/Ag reference electrode (not shown) and is clearly distinct from the polarograms of α-$[SiW_9O_{34}]^{10-}$ (one wave of 4e at –0.79 V) or α-$[SiW_{11}O_{39}]^{8-}$ (two waves of 2e at –0.73 and –0.90 V) in the same medium.[21] Titration experiments carried out on a solution of **H_2-1** between pH = 1.5 and 12.5 (see Figure 3) revealed the transfer of three protons at pKa ≈ 3.5, 4.8 and 9.8, consistent with the existence of four possible protonation states for the sandwiched zirconium cluster $\{H_xZr_3O_3\}$ with x = 3, 2, 1 or 0.

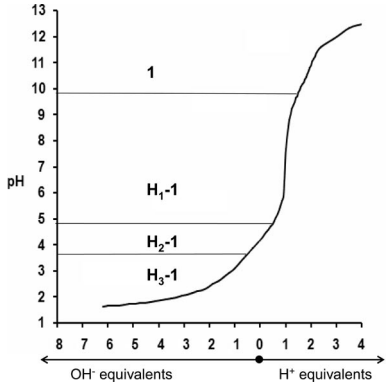

Figure 3. pH titration curve of **H_2-1** showing the predominating domains of the **H_x-1** species.

Infrared Spectroscopy. The infrared spectra of **NaCs-H_x-1** are very similar and exhibit the characteristic features of Keggin-type POMs (see Figure 4 and Exp. Sect. for the IR data). The presence of zirconium atoms seems to be related to a medium absorption observed at ca. 700 cm^{-1} (see Figure 4). According to reported results, the Zr–O(H)–Zr stretching modes appear in the 700–800 cm^{-1} range. In the complex $\{[ZrW_5O_{18}(\mu\text{-}OH)]_2\}^{6-}$, in which the two Linqvist subunits are attached through a double hydroxo bridge, the Zr–OH–Zr band can be observed at 728 cm^{-1} while in a similar dimeric arrangement reported by Khooldeeva et al. involving two bridged $[PW_{11}O_{39}]^{7-}$ moieties, the Zr–OH–Zr stretching mode is mentioned at higher energy (785 cm^{-1}). Such variations could be related to the Zr–OH–Zr geometric parameters such as the Zr–O bond lengths or the Zr–OH–Zr angles. Furthermore, the vibrational coupling be-

tween the Zr–OH–Zr bridges and the polyoxotungstate framework should also be considered. The magnitude of such coupling should be mainly dependent on the W–O–Zr angles. Thus, the opening of the Zr–OH–Zr or the W–O–Zr angles should induce an increase in the Zr–OH–Zr angle. Successive protonation of the $\{Zr_3O_3\}$ core within **1** leads to a slight gradual decrease of the involved absorption observed at 709, 695 and 690 cm^{-1} for $\mathbf{H_1}$-**1**, $\mathbf{H_2}$-**1** and $\mathbf{H_3}$-**1**, respectively. Such variations appear to be consistent with an increase of the Zr–O distances accompanied by the closing of the Zr–O–Zr angles, both provoked by the presence of a proton on the bridging oxygen atom.

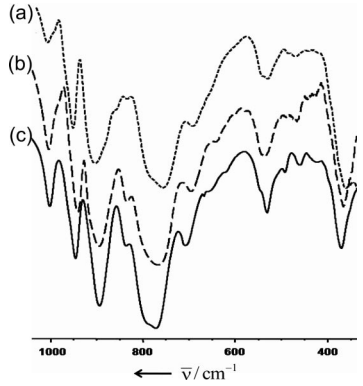

Figure 4. Infrared spectra of $\mathbf{H_3}$-**1** (a), $\mathbf{H_2}$-**1** (b) and $\mathbf{H_1}$-**1** (c) as mixed sodium/cesium salts (**NaCs-H$_x$-1**).

^{29}Si and ^{183}W NMR Spectroscopy. The ^{29}Si NMR spectra of $\mathbf{H_x}$-**1** (x = 1, 2 or 3) were recorded on concentrated solutions of the corresponding sodium salt (0.1–0.2 mol L^{-1}). The ^{29}Si NMR spectra shown in Figure 5 consist of a single sharp signal consistent with two equivalent $\{SiW_9O_{34}\}$ subunits within each dimeric anion. The three signals exhibit similar linewidths ($\Delta\nu_{1/2} \approx 1.5$ Hz) but the protonation state manifests itself as a gradual deshielding of the ^{29}Si nuclei from –85.3 ppm in $\mathbf{H_1}$-**1** to –84.6 ppm in $\mathbf{H_3}$-**1**. The ^{29}Si chemical shifts are in the expected range for anions built upon the $\{A\text{-}\alpha\text{-}SiW_9O_{34}\}$ subunit.[22]

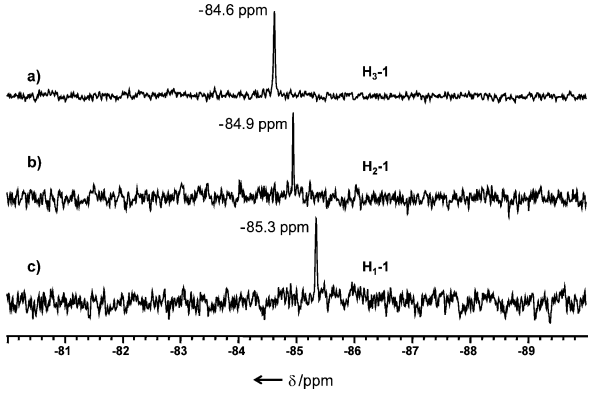

Figure 5. ^{29}Si NMR spectra of $\mathbf{H_3}$-**1** (a), $\mathbf{H_2}$-**1** (b) and $\mathbf{H_1}$-**1** (c) as Na^+ salts showing a single resonance at –84.6, –84.9 and –85.3 ppm, respectively.

The ^{183}W NMR spectra are shown in Figure 6 with the corresponding NMR spectroscopic data given in Table 1. ^{183}W NMR spectroscopy of the anion $\mathbf{H_2}$-**1** as its Na^+ salt in aqueous solution (Figure 6, b) gives a two-line spectrum with resonances at –151.4 and –161.4 ppm with a relative intensity of 2:1 in the usual chemical shift range observed for polyoxotungstate-based compounds. This feature, supported by the ^{29}Si NMR result, is consistent with an average D_{3h} symmetry for $\mathbf{H_2}$-**1** in solution. Both $\{SiW_9O_{34}\}$ subunits are equivalent and exhibit a C_{3v} local symmetry. The –151.4 ppm line can be attributed to the six W atoms of the belt and the resonance at –161.4 ppm to the three W atoms belonging to the cap (see Figure 1, a). Besides, the –151.4 ppm resonance appears significantly broadened ($\Delta\nu_{1/2}$ = 21 Hz) while the other at –161.4 ppm remains sharp ($\Delta\nu_{1/2}$ = 2.3 Hz). Seemingly, the increasing symmetry of the diprotonated anion $\mathbf{H_2}$-**1** from idealised C_{2v} to the averaged D_{3h} associated with the broadening of the 6 W-line is indicative of a moderately slow hopping of the two protons over the three bridging oxygens O(69,70,71). Such a dynamic process is clearly favoured by the fast exchange occurring between the attached protons and solvent (D_2O–H_2O). The shielded resonance (3 W signals at –161.4 ppm) exhibits coupling satellites ($^2J_{W\text{–}O\text{–}W}$ = 15.3 Hz) characteristic of corner junctions between the tungsten of the cap and those of the belt.[23–25] At lower pH values (pH ≈ 2), where the triprotonated species ($\mathbf{H_3}$-**1**) is preponderant, the resonance of the belt appears shielded by 4 ppm while that of the cap is deshielded slightly by 1.3 ppm. Moreover, the line width of the 6 W-line strongly sharpens ($\Delta\nu_{1/2}$ = 1.6 Hz), enabling the corner coupling to be observed on both signals ($^2J_{W\text{–}O\text{–}W}$ = 15.5 Hz). Interestingly, the ^{183}W NMR spectrum of the monoprotonated **H-1** species reveals only a single resonance at –162.2 ppm, associated with a doublet satellite ($^2J_{W\text{–}O\text{–}W}$ = 15.4 Hz). Several factors allow us to attribute this single resonance to the three W atoms of the cap: i) the relative intensity of the satellite peaks (≈ 14%) is consistent with the expected coupling scheme; ii) the chemical shift (–162.2 ppm) is close to those previously attributed to the three W atoms of the cap in $\mathbf{H_2}$-**1** (–161.4 ppm) and $\mathbf{H_3}$-**1** (–160.1 ppm). Then, the missing resonance should correspond to the six W atoms of the belts. Expected at about –147 ± 1 ppm (on the basis of a gradual deshielding upon deprotonation), this line is unobserved probably because of the dramatic increase of its line width. Unfortunately, our efforts to get the ^{183}W NMR spectrum of the unprotonated species failed. Although the potentiometric titration shows a last proton exchange at pK_a = 9.8, the unprotonated species **1** slowly decomposes during the ^{183}W NMR acquisition time to give several unresolved resonances (not shown). Nevertheless, the overall observations suggest that a dynamic process dependent upon the proton distribution occurs within the $\{Zr_3O_3\}$ core, substantially broadening the resonances of the tungsten atoms of the belt, connected to the Zr atom through W–O–Zr bridges but also to a lesser extent, those of the cap (see Table 1). In aqueous solution, two dynamic events involving H^+ ions have to be taken into account: i) the exchange be-

tween the attached H^+ and those of the solvent which is expected to proceed rapidly on the NMR timescale and should be nearly independent of the protonation state of the complex; ii) the "net" hopping of the H^+ ions over the oxygen atoms belonging to the Zr–O–Zr bridges which is assisted necessarily by the first exchange mechanism involving the solvent. The static model given by the crystallographic structure of **H_2-1** suggests that the H^+ mobility over the three Zr–O–Zr bridges produces local dynamic structural effects. Indeed, the protonated and unprotonated Zr–O–Zr bridges in **H_2-1** were clearly distinguished by characteristic bond lengths and angles which differ by about 7–8% (see above and Figure 2). Then, due to the H^+ hopping, structural relaxation of the $\{Zr_3O_3\}$ core must occur. For the **H_3-1** anion, the narrow ^{183}W peak widths in the NMR spectrum indicate that the three hydroxo groups are in the fast exchange limit on the NMR timescale. In such a configuration, "net" H^+ hopping cannot occur and only H^+ fast exchange between the anion and the solvent is involved. The ^{183}W resonances of the diprotonated **H_2-1** anion are broadened, featuring a moderately slow dynamic mechanism while the H^+ exchange with the solvent is expected to always proceed quickly. The main difference with the **H_3-1** anion lies in the possibility of "net" hopping of protons over the bridging oxygen atoms which gives rise to a subsequent structural relaxation. Thus, the rate of the H^+ hopping mechanism could be governed by a slow structural relaxation occurring within the $\{Zr_3O_3\}$ core. The slowness of such a dynamic structural effect from proton hopping could be related to the peculiar location of the $\{Zr_3O_3\}$ core (see Figure 1, b), closely embedded and compressed between both rigid $\{SiW_9O_{34}\}$ subunits (as noted previously by Finke[2]). Such a situation could strongly hamper the dynamic relaxation of the molecular framework and thus render slow the net H^+ hopping over the $\{Zr_3O_3\}$ triangle, even in aqueous solution. This feature contrasts with other POM systems such as monoprotonated $[SiW_9M_3O_{40}]^{n-}$ Keggin anions in aqueous solution in which the H^+ hopping over the $\{M_3O_3\}$ cap was found to proceed more quickly.[26] The H^+ hopping frequency decreases further within the monoprotonated anion **H_1-1** since the ^{183}W resonances still broaden, until those attributed to the belt ultimately vanish (see Figure 6, c). These results suggest that the dynamics of the relaxation process are dependent upon the protonation rate of the $\{Zr_3O_3\}$ fragment.

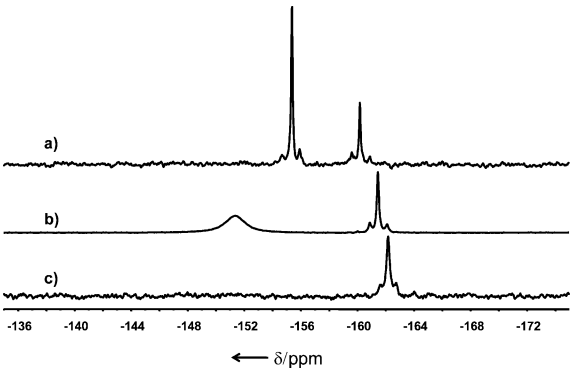

Figure 6. ^{183}W NMR spectra of **H_3-1** (a), **H_2-1** (b) and **H_1-1** (c) as Na^+ salts.

Table 1. ^{183}W-NMR spectroscopic data of **H_x-1** with x = 3, 2 or 1.

Compound	pH	δ (ppm) / $\Delta\nu_{1/2}$ (Hz) / $^2J_{W-O-W}$ (Hz)	
		belt	cap
H_3-1	2	–155.4/1.6/15.5	–160.1/1.5/15.5
H_2-1	4	–151.4/21/(*)	–161.4/2.3/15.3
H_1-1	7.5	(*)/(*)/(*)[a]	–162.2/3.4/15.4

[a] (*) unobserved.

In summary, we have synthesised a zirconium-containing sandwich-like complex based on two A-α-$[SiW_9O_{34}]^{10-}$ subunits and a central extra-belt $\{Zr_3O(OH)_2\}$ built up from one oxo and two hydroxo bridges. ^{183}W NMR studies in aqueous media reveal a slow H^+ hopping over the three Zr–O–Zr bridges which could be attributed to the peculiarity of the sandwich arrangement, hindering any structural relaxation within the $\{Zr_3O_3\}$ core.

Experimental Section

Synthesis: The lacunary ligand $K_{10}[SiW_9O_{34}]\cdot 13H_2O$ was prepared according to the literature method.[19]

$Na_6Cs_6[Zr_3O(OH)_2(SiW_9O_{34})_2]\cdot 31H_2O$ (CsNa-H_2-1): $K_{10}[SiW_9O_{34}]\cdot 13H_2O$ (9.3 g, 3.2 mmol) was suspended in water (260 mL) and then acidified with 1 mol L^{-1} HCl (6.4 mL) until pH = 6 was reached. To the clear solution, $ZrOCl_2\cdot 8H_2O$ (1.03 g, 3.2 mmol) was added inducing a decrease in the pH down to 4. After 30 min of stirring, CsCl (4.2 g; 25 mmol) was added and this caused the precipitation of a white solid (**CsK-1**). This solid was isolated by filtration and washed with EtOH and dried with Et_2O. 9 g of solid were collected (yield 88%). **CsK-1** (1 g) was dissolved in 0.7 mol L^{-1} NaCl aqueous solution (35 mL). After 4 d at room temperature, well-shaped colourless cubic crystals, suitable for X-ray diffraction analysis, were collected. (yield 0.2 g; 20%). $Na_6Cs_6[Zr_3O(OH)_2(SiW_9O_{34})_2]\cdot 31H_2O$ (**CsNa-H_2-1**) (6270.96): calcd. Zr 4.36, W 52.77, Si 0.93, Cs 12.72, Na 2.20; found Zr 4.33, W 50.97, Si 0.93, Cs 12.56, Na 1.80. IR (KBr pellet): $\tilde{\nu}$ = 1004 (w), 941 (m), 895 (s), 836 (m), 768 (s), 695 (m), 639 (w), 536 (w), 467 (w) cm^{-1}.

$Na_6Cs_5[Zr_3(OH)_3(SiW_9O_{34})_2]\cdot 28H_2O$ (CsNa-H_3-1): The synthetic procedure was similar to that used for **CsNa-H_2-1**. The white solid **CsK-1** (1 g) was dissolved in 0.7 mol L^{-1} NaCl (30 mL) with moderate heating (50 °C). A few drops of 1 mol L^{-1} HCl were then added until the pH was lowered to 2 and the solution was filtered. After 4–5 d at room temperature crystalline material was collected which was washed with EtOH and dried with Et_2O (yield 0.19 g; 20%). $Cs_5Na_6[Zr_3(OH)_3(SiW_9O_{34})_2]\cdot 28H_2O$ (**CsNa-H_3-1**) (6083.96): calcd. Zr 4.50, W 54.39, Si 0.95, Cs 10.93, Na 2.27; found Zr 4.44, W 53.51, Si 0.96, Cs 11.22, Na 2.12. IR (KBr pellet): $\tilde{\nu}$ = 1004 (w), 951 (m), 904 (s), 855 (sh), 831 (vw), 788 (sh), 756 (s), 690 (m), 543 (sh), 530 (w) cm^{-1}.

$Na_7Cs_6[Zr_3O_2(OH)(SiW_9O_{34})_2]\cdot 33H_2O$ (CsNa-H_1-1): CsNa-H_1-1 was obtained as crystalline material from the white solid **CsK-1**. **CsK-1** (1 g) was dissolved at 50 °C in 0.7 mol L^{-1} NaCl solution (30 mL). The pH was adjusted up to 7.5 by addition of a few drops

of 1 mol L^{-1} NaOH. The solution was allowed to stand at room temperature for 4 d. Crystalline material was then collected, washed with EtOH and dried with Et_2O (yield 0.23 g; 23%). $Na_7Cs_6[Zr_3O_2(OH)(SiW_9O_{34})_2]\cdot 33H_2O$ (**CsNa-H$_1$-1**) (6329.96): calcd. Zr 4.32, W 52.28, Si 0.92, Cs 12.61, Na 2.54; found Zr 4.11, W 51.68, Si 0.93, Cs 12.94, Na 2.27. IR (KBr pellet): $\tilde{\nu}$ = 1002 (w), 946 (m), 895 (s), 836 (w), 795 (sh), 773 (vs), 695 (m), 709 (m), 546 (sh), 531 (m) cm^{-1}.

The ^{29}Si NMR measurements were carried out on solutions of **Na-H$_x$-1**, obtained from the corresponding mixed sodium-cesium salts (**CsNa-H$_x$-1**) by cationic exchange. **CsNa-H$_x$-1** compounds (1.5–2 g) were suspended in water (25 mL) and treated with an Na^+ resin (Dowex 50–80). The resultant solutions were evaporated to dryness. The solid formed in each case was dissolved in 70:30 (v/v) H_2O/D_2O mixture (2 mL) to give an approximately 0.13–0.17 mol L^{-1} NMR sample.

The ^{183}W NMR samples of the anions **H$_3$-1** and **H-1** were obtained from the crystalline compound **CsNa-H$_2$-1**. The starting procedure was similar. After cationic exchange through an Na^+ Dowex 50–80 resin, a 6.4×10^{-3} mol L^{-1} solution of **H$_2$-1** was acidified with 1 mol L^{-1} HCl solution until a pH = 2 was reached or, alternatively, treated with 1 mol L^{-1} NaOH solution (0.25 mL, 1 equiv. of OH^-; pH = 7.5) to give the corresponding **H$_3$-1** and **H-1** solutions, respectively. The concentrated ^{183}W NMR samples of **H$_3$-1** and **H$_1$-1** were then obtained from these solutions using a similar procedure as that used for the **H$_2$-1** sample.

Time-averaged ^{183}W FT NMR (12.5 MHz) spectra were recorded on a Bruker Avance 300 MHz spectrometer (25 °C, 10 mm sample tube). Chemical shifts were referenced to the ^{183}W resonance of an external 2 M Na_2WO_4 solution in alkaline D_2O and to dodecatungstosilicic acid as a secondary standard (δ = –103.8 ppm). ^{29}Si NMR (79.5 MHz) spectra were recorded on a Bruker Avance 400MHz spectrometer (25 °C, 5 mm sample tube) and ^{29}Si chemical shifts were referenced to TMS.

X-ray Crystallography: A single-crystal of compound **CsNa-H$_2$-1** was mounted on a glass fibre for indexing and intensity data collection at 293 K on a Bruker X8-APEX2 CCD area-detector diffractometer using Mo-K_α radiation (λ = 0.71073 Å). Six sets for 1 of narrow data frames (45 s per frame for 1) were collected at different values of θ (for 2 and 4 initial values of ϕ and ω for 1) using 0.5° increments of ϕ or ω.

Crystal data and structure refinements for **CsNa-H$_2$-1**: Colourless crystal, dimensions $0.15\times0.10\times0.08$ mm, triclinic, space group $P\bar{1}$, a = 13.162(2), b = 15.674(2), c = 24.783(3) Å, α = 89.060(6)°, β = 88.751(6)°, γ = 80.586(6)°, V = 5042.7(9) Å^3, Z = 2, $\rho_{calcd.}$ = 4.148 g cm^{-3}, μ(Mo-K_α) = 23.121 mm^{-1}, F(000) = 5534, T = 293(2) K. A total of 29324 independent reflections, 18805 observed with $I > 2\sigma(I)$, R(int) = 0.098, R_1 = 0.082, wR_2 = 0.218, 1165 refined parameters.

Data reduction was accomplished using SAINT V7.03.[27] The substantial redundancy in data allowed a semi-empirical absorption correction (SADABS V2.10)[27] to be applied on the basis of multiple measurements of equivalent reflections. The structure was solved by direct methods, developed by successive difference Fourier syntheses and refined by full-matrix least-squares on all F^2 data using SHELXTL V6.14.[28]

CSD-419145 (for **CsNa-H$_2$-1**) contains the supplementary crystallographic data for this paper. This material can be obtained from the Fachinformationszentrum Karlsruhe, Abt. PROKA, 76344 Eggenstein-Leopoldshafen, Germany (Fax: +49-7247-808-666; E-mail: crysdata@fiz-karlsruhe.de), on quoting the depository number .

[1] a) M. T. Pope, *Heteropoly and Isopoly Oxometalates*; Springer: Berlin, **1983**; b) M. T. Pope, *Comprehensive. Coord. Chem. II* **2003**, *4*, 635; c) C. L. Hill, *Comprehensive. Coord. Chem. II* **2003**, *4*, 679; d) *Polyoxometalate Molecular Science* (Eds.: J. J. Borrâs-Almenar, E. Coronado, A. Müller, M. T. Pope), Kluwer, Dordrecht, The Netherlands, **2004**; e) *Polyoxometalates: from Platonic Solids to Anti Retroviral Activity* (Eds.: M. T.Pope, A. Müller), Kluwer, Dordrecht, The Netherlands, **1994**; f) *Chem. Rev.* **1998**, 98, 1–389 (Special Thematic Issue on Polyoxometalates); g) *Polyoxometalate Chemistry: From Topology via Self-Assembly to Applications* (Eds.: M. T. Pope, A. Müller), Kluwer, Dordrecht, The Netherlands, **2001**; h) *Polyoxometalate Chemistry for Nano-Composite Design* (Eds.: T. Yamase, M. T. Pope), Kluwer, Dordrecht, The Netherlands, **2002**; i) L.-H. Bi, U. Kortz, S. Nellutla, A. C. Stowe, J. van Tol, N. S. Dalal, B. Keita, L. Nadjo, *Inorg. Chem.* **2005**, *44*, 896; j) B. Godin, Y.-G. Chen, J. Vaissermann, L. Ruhlmann, M. Verdaguer, P. Gouzerh, *Angew. Chem. Int. Ed.* **2005**, *44*, 3072; k) B. Godin, J. Vaissermann, P. Herson, L. Ruhlmann, M. Verdaguer, P. Gouzerh, *Chem. Commun.* **2005**, 5624; l) I. M. Mbomekalle, B. Keita, L. Nadjo, W. A. Neiwert, L. Zhang, K. I. Hardcastle, C. L. Hill, T. M. Anderson, *Eur. J. Inorg. Chem.* **2003**, 3924; m) T. M. Anderson, X. Zhang, K. I. Hardcastle, C. L. Hill, *Inorg. Chem.* **2002**, *41*, 2477; n) U. Kortz, M. G. Savelieff, B. S. Bassil, B. Keita, L. Nadjo, *Inorg. Chem.* **2002**, *41*, 783; o) A. Tézé, J. Vaissermann, *C. R. Acad, Sci. Paris* **2000**, *3*, 101; p) M.-X. Li, S.-L. Jin, H.-Z. Liu, G.-Y. Xie, M.-Q. Chen, Z. Xu, X.-Z. You, *Polyhedron* **1998**, *17*, 3721; q) C. Nozaki, I. Kiyoto, Y. Minai, M. Misono, N. Mizuno, *Inorg. Chem.* **1999**, *38*, 5724.

[2] R. G. Finke, B. Rapko, T. J. R. Weakley, *Inorg. Chem.* **1989**, *28*, 1573.

[3] O. A. Kholdeeva, R. I. Maksimovskaya, *J. Mol. Catal. A* **2007**, *262*, 7.

[4] a) S. Loridant, C. Feche, N. Essayem, F. Figueras, *J. Phys. Chem., Part B* **2005**, *109*, 5631–5637, b) I. E. Wachs, T. Kim, E. I. Ross, *Catal. Today* **2006**, *116*, 162–169; c) T. Kim, A. Burrows, C. J. Kiely, I. E. Wachs, *J. Catal.* **2007**, *246*, 370–381; d) A. Martiny, G. Prieto, M. A. Arribas, P. Conception, J. F. Sanchez-Royo, *J. Catal.* **2007**, *248*, 288–302.

[5] N. C. Kato, A. Shinora, K. Hayashi, K. Nomiya, *Inorg. Chem.* **2006**, *45*, 8108.

[6] A. J. Gaunt, I. May, D. Collison, O. D. Fox, *Inorg. Chem.* **2003**, *42*, 5049.

[7] B. S. Bassil, M. H. Dickman, U. Kortz, *Inorg. Chem.* **2006**, *45*, 2394.

[8] A. J. Gaunt, I. May, D. Collison, K. T. Holman, M. T. Pope, *J. Mol. Struct.* **2003**, *656*, 101.

[9] X. Fang, T. M. Anderson, C. L. Hill, *Angew. Chem. Int. Ed.* **2005**, *44*, 3540.

[10] X. Fang, T. M. Anderson, Y. Hou, C. L. Hill, *Chem. Commun.* **2005**, 5044.

[11] X. Fang, C. L. Hill, *Angew. Chem. Int. Ed.* **2007**, *46*, 3877.

[12] a) R. Villaneau, H. Carabieiro, X. Carrier, R. Thouvenot, P. Herson, F. Lemos, F. R. Ribeiro, M. Che, *J. Phys. Chem. B* **2004**, *108*, 12465–12471; b) H. Carabineiro, R. Villaneau, X. Carrier, P. Herson, F. Lemos, F. Ribeiro, A. Proust, M. Che, *Inorg. Chem.* **2006**, *45*, 1915–1923.

[13] O. A. Kholdeeva, G. M. Maksimov, R. I. Maksimovskaya, M. P. Vanina, T. A. Trubitsina, D. Y. Naumov, B. A. Kolesov, N. S. Antonova, J. J. Carbo, J. M. Poblet, *Inorg. Chem.* **2006**, *45*, 7224.

[14] A. J. Gaunt, I. May, D. Collison, M. Helliwell, *Acta Crystallogr., Sect. C* **2003**, *59*, i65.

[15] R. J. Errington, S. S. Petkar, P. S. Middleton, W. McFarlane, W. Clegg, R. A. Coxall, R. W. Harrington, *J. Am. Chem. Soc.* **2007**, *129*, 12181–12196.
[16] N. Laronze, J. Marrot, G. Hervé, *Chem. Commun.* **2003**, 2360.
[17] N. Leclerc-Laronze, J. Marrot, G. Hervé, *Inorg. Chem.* **2005**, *44*, 1275.
[18] N. Leclerc-Laronze, J. Marrot, G. Hervé, *C. R. Chim.* **2006**, *9*, 1467.
[19] N. Laronze, J. Marrot, G. Hervé, *Inorg. Chem.* **2003**, *42*, 5857.
[20] W. H. Knoth, P. J. Domaille, R. L. Harlow, *Inorg. Chem.* **1986**, *25*, 1577.
[21] a) G. Herve, A. Teze, *Inorg. Chem.* **1977**, *16*, 2115–2117; b) A. Teze, G. Herve, *J. Inorg. Nucl. Chem.* **1977**, *39*, 999–1002.
[22] a) N. Leclerc-Laronze, M. Haouas, J. Marrot, F. Taulelle, G. Herve, *Angew. Chem. Int. Ed.* **2006**, *45*, 139–142; b) C. R. Mayer, I. Fournier, R. Thouvenot, *Chem. Eur. J.* **2000**, *6*, 105–110
[23] a) R. Acerete, C. F. Hammer, L. C. W. Baker, *Inorg. Chem.* **1984**, *23*, 1478; M. Kozik, C. F. Hammer, L. C. W. Baker, *J. Am. Chem. Soc.* **1986**, *108*, 2748; M. Kozik, C. F. Hammer, L. C. W. Baker, *J. Am. Chem. Soc.* **1986**, *108*, 7627; M. Kozik, L. C. W. Baker, *J. Am. Chem. Soc.* **1987**, *109*, 3159; T. L. Jorris, M. Kozik, N. Casan-Pastor, P. J. Domaille, R. G. Finke, W. K. Miller, C. L. W. Baker, *J. Am. Chem. SOC.* **1987**, *109*, 7402; b) P. J. Domaille, *J. Am. Chem. Soc.* **1984**, *106*, 7677 and references cited therein; c) W. H. Knoth, P. J. Domaille, D. C. Roe, *Inorg. Chem.* **1983**, *22*, 198; d) W. H. Knoth, P. J. Domaille, R. D. Farlee, *Organometallics* **1985**, *4*, 62; e) R. G. Finke, M. W. Droege, *J. Am. Chem. Soc.* **1984**, *106*, 7274.
[24] a) R. G. Finke, M. Droege, J. R. Hutchinson, O. A. Ganzow, *J. Am. Chem. Soc.* **1981**, *103*, 1587; b) R. G. Finke, M. W. Droege, *Inorg. Chem.* **1983**, *22*, 1006; c) R. G. Finke, B. Rapko, P. J. Domaille, *Organometallics* **1986**, *5*, 175.
[25] a) J. Lefebvre, F. Chauveau, P. Doppelt, C. Brevard, *J. Am. Chem. Soc.* **1981**, *103*, 4589; b) P. J. Domaille, W. H. Knoth, *Inorg. Chem.* **1983**, *22*, 818; c) C. Brevard, R. Schimpf, G. Tourné, C. Tourné, *J. Am. Chem. Soc.* **1983**, *105*, 7059; d) However, one exception to this use of $^2J_{w-o-w}$ coupling constant correlation to edge- vs. corner-sharing octahedral linkage has been reported[25c] e) J. Canny, A. Tézé, R. Thouvenot, G. Hervé, *Inorg. Chem.* **1986**, *25*, 2114.
[26] R. G. Finke, B. Roko, R. J. Saxton, P. J. Domaille, *J. Am. Chem. Soc.* **1986**, *108*, 2947–2960.
[27] *APEX2*, version 1.0-8, Bruker AXS, Madison, WI, **2003**.
[28] *SHELXTL*, version 6.14, Bruker AXS, Madison, WI, **2001**.

Received: February 29, 2008
Published Online: September 25, 2008

